

How Dense is Ultra-Dense for Wireless Networks: From Far- to Near-Field Communications

Junyu Liu, Min Sheng, Lei Liu, Jiandong Li

State Key Laboratory of Integrated Service Networks, Xidian University, Xi'an,
Shaanxi, 710071, China

Email: {jyliu, leiliu}@stu.xidian.edu.cn, {msheng, jdli}@mail.xidian.edu.cn

Abstract

Besides advanced telecommunications techniques, the most prominent evolution of wireless networks is the densification of network deployment. In particular, the increasing access points/users density and reduced cell size significantly enhance spatial reuse, thereby improving network capacity. Nevertheless, does network ultra-densification and over-deployment always boost the performance of wireless networks? Since the distance from transmitters to receivers is greatly reduced in dense networks, signal is more likely to be propagated from far- to near-field region. Without considering near-field propagation features, conventional understandings of the impact of network densification become doubtful. With this regard, it is imperative to reconsider the pros and cons brought by network densification. In this article, we first discuss the near-field propagation features in densely deployed network and verify through experimental results the validity of the proposed near-field propagation model. Considering near-field propagation, we further explore how dense is ultra-dense for wireless networks and provide a concrete interpretation of ultra-densification from the spatial throughput perspective. Meanwhile, as near-field propagation makes interference more complicated and difficult to handle, we shed light on the key challenges of applying interference management in ultra-dense wireless networks. Moreover, possible solutions are presented to suggest future directions.

I. INTRODUCTION

Instead of the enhancement of radio access networks (RANs), the future wireless networks are more likely to act as a mixture of various types of RANs, e.g., macro-cell base stations (BSs), femto-cell BSs, pico-cell BSs and WiFi access points (APs), etc. By 2030, the targets are to support ubiquitous device connectivity and expand network capacity, including 100 billion device connectivities, $20000\times$ mobile data traffic and $1000\times$ user experienced data rate, etc., compared to 2010 [1]. The requirements are even more critical for popular scenarios. For instance, tens of Tbps/km² is required in the office, 1 million connections/km² is required at densely populated areas such as stadium and open gathering, and super high density of over 6 persons/m² is to be supported in subways. Among the appealing approaches to realize the ambitious goals, network densification is shown to be the most promising one, which has improved network capacity by 2700 folds from 1950 to 2000 [2]. The principle of network densification is to deploy BSs/APs with smaller coverage and enables local spectrum reuse. In consequence, users can be served with shorter transmission links, thereby fully exploiting spatial and spectral resources.

However, does aggressively deploying more BSs and devices always improve the system performance? As network densification significantly reduces transmission distance and enables proximity communication, the signal propagation may transit from far- to near-field propagation. For instance, as shown in Table I, if the BS density is increased from 1 BS/km² to 100 BS/km², the average transmission link length is reduced 10 folds from 500 m to 50 m, which makes a larger proportion of downlink users located within the near-field propagation distance. Meanwhile, the application of device-to-device (D2D) communications allows direct local transmission of nearby users to bypass centralized BSs, which greatly shortens the distance between transmitters (Tx's) and the potential receivers (Rx's) as well. Since signal strength is moderately attenuated within the near-field region, desired signal strength is greatly enhanced compared to far-field transmission. However, in traditional wireless communications system, the performance evaluation and protocol design are basically based on the assumption of far-field transmission. Therefore, the impact of network densification and near-field transmission on wireless network performance remains to be explored.

Avg. of link length d (m)	BS density (BS/km ²)	$P(d < 1 \text{ m})$	Band 2 (Downlink, 1.93 - 1.99 GHz) of AT&T, $P(d < \bar{R}_{F,1} = 29.45 \text{ m})$	Band 4 (Downlink, 2.11 - 2.155 GHz) of Verizon, $P(d < \bar{R}_{F,2} = 13.1 \text{ m})$	Band 38 (Downlink, 2.57 - 2.62 GHz) of CMCC, $P(d < \bar{R}_{F,3} = 3.25 \text{ m})$
500	1	3.1×10^{-6}	0.27%	0.05%	0.03‰
100	25	0.08‰	6.6%	1.3%	0.08%
50	100	0.03%	23.9%	5.2%	0.3%
10	2500	0.8%	99.9%	73.5%	7.7%
5	10000	17.8%	$\approx 100\%$	99.5%	27.5%
1	250000	54.4%	$\approx 100\%$	$\approx 100\%$	$\approx 100\%$

Table I. The probability that transmission link distance is within Fraunhofer distance, the boundary between near- and far-field regions, under typical settings. 1) For Band 2 of AT&T and antenna size $D = 1.5$ m, the Fraunhofer distance is $R_{F,1} = 29.0 - 29.9$ m. 2) For Band 4 of Verizon and antenna size $D = 1$ m, the Fraunhofer distance is $R_{F,2} = 12.9 - 13.3$ m. 3) For Band 38 of CMCC and antenna size $D = 0.5$ m, the Fraunhofer distance is $R_{F,3} = 3.2 - 3.3$ m. Note that $\bar{R}_{F,1}$, $\bar{R}_{F,2}$ and $\bar{R}_{F,3}$ denote the average of $R_{F,1}$, $R_{F,2}$ and $R_{F,3}$, respectively. The statistics are obtained provided that users are connected to the geometrically nearest BSs.

Recently, the research of densely deployed wireless networks has gained great attention from both academia and industries, including architecture development [3], [4], analytical studies [5], [6] and protocol design [7], [8]. Remarkably, a user-centric architecture has been presented for ultra-dense networks (UDN) [4], under which functions such as mobility management, resource management and interference management, can be co-designed and jointly optimized. Meanwhile, to comprehensively understand the merits and limits brought by network densification, authors study the network capacity scaling law in downlink cellular network [5], [6]. Wherein, the impact of both line-of-sight (LoS) and non-LoS (NLoS) transmissions has been fully explored. Depending on parameters, it is shown that the spatial throughput, which is an indicator of network capacity, scales slowly and even diminishes to be zero when BS density is sufficiently large [5]. The above results indicate that network densification may be beneficial, while network ultra-densification would lose the merits of network capacity enhancement when spatial resources are fully exhausted. Nevertheless, despite the progress achieved by recent research, there is still no consensus on how dense is ultra-dense in wireless networks. More importantly, the available study fails to capture the influence of near-field transmissions in UDN, which makes the existing results dubious and doubtful.

With this regard, we intend to characterize ultra-densification for wireless networks by fully exploring near-field propagation features. To this end, we first provide answers to the following two questions: 1) how to characterize near-field propagation features and 2) how near-field propagation influences the performance of wireless networks in terms of spatial throughput. Aided by the spatial throughput scaling law, we then concretely reveal how dense is ultra-dense in wireless networks. Besides, as near-field propagation complicates interference distribution, which may bottleneck the performance of UDN, new opportunities are provided for interference management techniques. Concerning this, we highlight key challenges and potential solutions to facilitate interference management in UDN. As an example, a tailored interference-cancellation-alignment (ICA) strategy is proposed by flexibly combining the advantages of successive interference cancellation (SIC) and interference alignment (IA).

The rest of this article is organized as follows. We first discuss signal propagation in the near- and far-field regions. Then, the interpretation of ultra-densification is presented from the spatial throughput scaling perspective. Following that, we focus on the open challenges brought by ultra-densification and possible solutions are provided as well, including the detail of the proposed interference management strategy. Finally, conclusion remarks are drawn.

II. NEAR-FIELD PROPAGATION IN UDN

As network densification would enable signals to propagate from far- to near-field region, what is the fundamental difference between near- and far-field propagation? To shed light on this, we discuss near-field propagation features in this part, based on which a multi-slope bounded pathloss model (BPM) is introduced to serve as the pathloss model¹ in UDN.

A. From Far-field Propagation to Near-field Propagation

Network densification would push Tx's and Rx's closer to each other. As a result, more Rx's are likely to be located within near-field regions of the associated Tx's. For instance, it is shown

¹It's worth noting that signal propagation is generally influenced by distance-dependent component, i.e., pathloss, and distance-independent components, e.g., shadowing and multi-path (small-scale) fading. In this article, we primarily focus on how the distance-dependent component varies with propagation distance, which is greatly reduced by network densification.

in Table I that this probability raises 88 folds from 0.27% to 23.9% when BS density increases from 1 BS/km² to 100 BS/km² under Band 2 of AT&T and antenna size $D = 1.5$ m. If BS density further increases from 1 BS/km² to 2500 BS/km², this probability astonishingly raises 1470 folds from 0.05% to 73.5% under Band 4 of Verizon and antenna size $D = 1$ m. This is especially true for scenarios like offices and dining halls, etc. For more crowded places, such as stadiums, more dense BS/AP deployment is required such that transmission distance is further reduced. We see from Table I that almost all the transmissions occur within near-field region when the BS density reaches 250000 BS/km² under the three typical settings. Therefore, to better understand the impact of network densification, it is essential to figure out signal propagation features over different propagation distance.

Considering cellular downlink transmissions, we introduce near- and far-field signal propagation regions for electromagnetically long antennas, which are physically larger than a half-wavelength of the radiation they emit. Denote λ , D , h_{Tx} and h_{Rx} as the signal wavelength, the largest dimension of Tx antennas, Tx and Rx antenna heights, respectively.

1) *Reactive near-field region* ($0 \sim R_{\text{B}}$): The region within $R_{\text{B}} = \frac{\lambda}{2\pi}$ from antenna is termed reactive near-field region, where the signal energy is held back and stored very near the antenna surface. Hence, signal power decays slowly with distance within this region.

2) *Radiative near-field region* ($R_{\text{B}} \sim R_{\text{F}}$): The region covering from $R_{\text{B}} = \frac{\lambda}{2\pi}$ to $R_{\text{F}} = \frac{2D^2}{\lambda}$ (Fraunhofer distance) is termed radiative near-field region, which, however, cannot efficiently store and replace inductive or capacitive energy from antenna currents or charges. This leads to slightly faster attenuation of signal power.

3) *Far-field region* ($R_{\text{F}} \sim \infty$): The region, which is $R_{\text{F}} = \frac{2D^2}{\lambda}$ or farther away from the antenna, is the far-field region. Wherein, absorption of the radiation does not feedback to the transmitter and radiation decreases as the square of distance. For this reason, signal power decays inversely proportional to the propagation distance of several orders. Considering short-range signal propagation within the far-field region, the two-ray model can suitably describe the two-ray ground reflection, where a critical distance $R_{\text{C}} = \frac{4h_{\text{Tx}}h_{\text{Rx}}}{\lambda}$ exists. In particular, the LoS and reflected components of signals cause constructive-destructive wave interference effects [9],

which makes the pathloss exponent within R_C smaller than that of free space. In contrast, out of R_C , the LoS and reflected waves add either constructively or destructively, which makes the pathloss exponent closer to that of free space.

To sum up, the signal strength first flattens out (in near-field region) and then rapidly decays (fast from R_F to R_C and faster beyond R_C in far-field region) with the propagation distance. The above propagation properties also apply to electromagnetically short antennas².

According to the above discussion, to model signal propagation in UDN, it is crucial to accurately capture the characteristics of channel gain within different propagation regions. Combining the available results in literature [5], [10], [11], we propose to use multi-slope BPM

$$g_N^B(\{\alpha_n\}_{n=0}^{n=N-1}; d) = \eta_n (1 + d^{\alpha_n})^{-1}, R_n < d \leq R_{n+1}, \quad (1)$$

where d denotes the distance from Tx to Rx, R_n denotes critical distance and α_n denotes the pathloss exponent for $R_n < d \leq R_{n+1}$. Meanwhile, $\eta_0 = 1$ and $\eta_n = \prod_{i=1}^n \frac{1+R_i^{\alpha_i}}{1+R_i^{\alpha_i-1}}$ are defined to maintain continuity of (1)³. Besides capable of capturing the near-field transmission features, the multi-slope model in (1) can be applied into different scenarios.

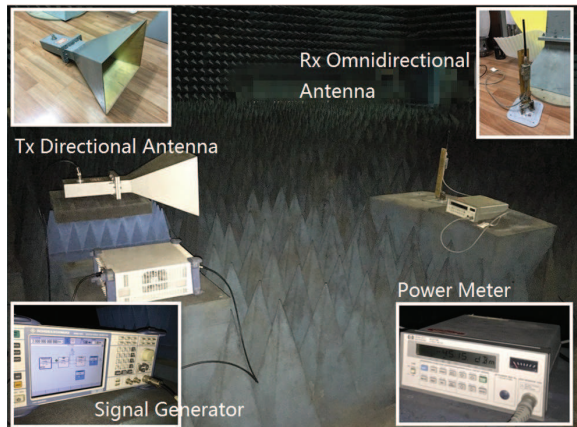
1) *Sparse outdoor scenarios*: When $N = 1$, (1) degenerates into the *single-slope BPM*, where one pathloss exponent is used to characterize the power decay rate in the free space. Therefore, the model is suitable for the sparse scenarios, where Tx's are basically located apart from Rx's.

2) *Dense outdoor scenarios*: When $N = 2$, (1) degenerates into the *dual-slope BPM*, where two pathloss exponents are used within and out of the critical distance. Therefore, this model can be applied in dense outdoor scenarios such as stadium and open gatherings, where Tx's and Rx's are located close to each other and there are signal LoS and reflected components.

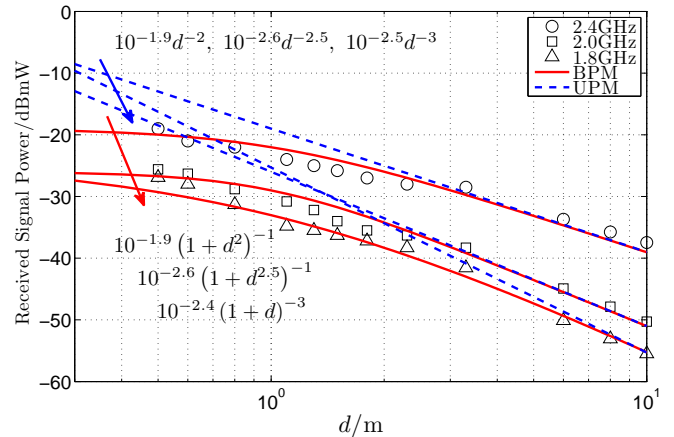
3) *Dense indoor scenarios*: When $N > 2$, multiple pathloss exponents are used to capture the discrepant power decay rates within different transmission distances. This is especially true for the indoor scenarios, where signals from different floors and regions may be attenuated with different rates.

²For electromagnetically short antennas, the difference is how to distinguish the near- and far-field region.

³Other rational BPMs could be in forms like $(1 + d)^{-\alpha_n}$ and $\min(1, d^{-\alpha_n})$. The form $(1 + d^{\alpha_n})^{-1}$ used in this article is a typical one, which has been widely applied in [10]–[12].



(a) Experimental scenarios.



(b) Experimental and fitting results.

Figure 1. Experimental results of received signal power for near-field transmission. In (b), markers denote the experimental results and lines denote the fitting results. Transmit power of the signal generator is set to be 0 dBmW.

B. Experimental Results of Short-Range Signal Propagation

In this part, we use experimental results to illustrate how received signal power varies with transmission distance especially in the near-field region. To avoid the influence of ambient interference signals generated by nearby cellular BSs and WiFi APs, the measurement is performed in an anechoic chamber of more than 1000 m², as shown in Fig. 1a. Meanwhile, the Tx directional antenna is connected to a Rohde & Schwarz SMBV100A Vector Signal Generator and the Rx omnidirectional antenna is connected to an HP-437B power meter. Signal carrier frequencies are set to be 1.8 GHz, 2.0 GHz and 2.4 GHz, respectively. Accordingly, the corresponding signal wavelengths are 0.167 m, 0.15 m and 0.125 m, respectively. Since the physical dimension of the Tx directional antenna is 0.5 m, which is greater than the half-wavelengths, the boundaries of the near- and far-field region are the Fraunhofer distances 3 m, 3.33 m and 4 m. Hence, signal power decay caused by near-field propagation can be reflected using the results in Fig. 1b.

In Fig. 1b, we evaluate the accuracy of BPM and unbounded pathloss model (UPM) in modeling how channel power gain decays with distance. Note that UPM has been widely applied as the pathloss model in sparse scenarios for its simplicity and mathematical tractability [5], [6], [13]. Typical single-slope UPM is $d^{-\alpha}$, where d and α denote transmission distance and pathloss

exponent, respectively. However, it can be seen from Fig. 1b that large gaps exist between the experimental results and fitting results when d is small under UPMs. In contrast, the gaps between the two results are relatively small even when single-slope BPMs are used (due to the small propagation distance). Besides, when d becomes larger, both BPMs and UPMs can well characterize the power loss. Therefore, the results are sufficient to indicate the rationality of using BPM to model channel power gain especially within near-field regions.

C. The Impact of Near-Field Propagation

With the knowledge of how to model near-field propagation, the problem lying ahead is how near-field propagation impacts wireless network performance.

Indeed, the influence of near-field propagation scales with network density, as large proportion of transmission links are within the near-field region and even 1 m in densely deployed networks. For example, as shown in Table I, when the BS density is 10000 BS/km², 17.8% Tx's transmit data to their Rx's within 1 m and, when the BS density further reaches 250000 BS/km², more than half of the Tx's complete data transmission within 1 m. This is especially true for the future Internet of Things (IoT) and indoor scenarios such as office, subway and shopping mall, etc.

Although UPM has been extensively used in sparse scenarios, the application of UPM would artificially make the received signal power greater than the transmitted signal power when $d \in [0, 1]$ m. For instance, under $d^{-\alpha}$ with $\alpha = 4$, if the transmission distance $d = 0.5$, Rx power would be 16 folds of the Tx power. This is apparently inconsistent with the actual situation. Therefore, neglecting the imprecision of UPM in modeling pathloss within the near-field region would lead to inaccuracy in the performance evaluation and protocol design. Particularly, considering near-field propagation, the conclusion that spatial throughput scales linearly/sublinearly with BS density in cellular networks [5], [6] may be totally overturned. Instead, network ultra-densification would eventually drain the spatial reuse and render network capacity diminishing to be zero. We will discuss the detail in the next part.

III. HOW DENSE IS ULTRA-DENSE

Although ultra-densification is a growing trend for the future wireless networks, there is still no consensus on how dense is ultra-dense. To answer the question, in this part, we show some of our recent results on the spatial throughput of wireless networks and give the interpretation of ultra-densification from the perspective of spatial throughput scaling law.

We define spatial throughput as follows:

$$\mathcal{ST} = \mu \mathbb{P}(\text{SINR} > \tau) \log(1 + \tau), \quad [\text{bits}/(\text{s} \cdot \text{Hz} \cdot \text{m}^2)] \quad (2)$$

where μ denotes the density of active links, τ denotes the signal-to-noise-and-interference ratio (SINR) threshold and $\mathbb{P}(\text{SINR} > \tau)$ denotes the success probability of data transmissions.

Intuitively, interference may degrade the SINR and the corresponding transmission success probability especially when μ is large, thereby serving as a limiting factor to spatial throughput. Meanwhile, considering near-field propagation, the interference distribution becomes complicated. Therefore, we first look into the features of interference in wireless networks by comparing sparse and dense scenarios.

A. Interference Distribution in Wireless Networks

Fig. 2 shows the interference level, considering sparse deployment (see Figs. 2a, 2b and 2c) and dense deployment (see Figs. 2d, 2e and 2f) of Tx's. Single-slope UPM, dual-slope UPM and dual-slope BPM serve as the pathloss models in Figs. 2a and 2d, Figs. 2b and 2e, and Figs. 2c and 2f, respectively.

We observe that, except for interference levels, the interference has similar distributions in Figs. 2a, 2b and 2c. Therefore, little difference exists in using bounded and unbounded model to characterize channel gain in sparse networks. Nevertheless, when the user density is high, we notice that the difference in the interference distribution is evident under different channel models. To be specific, despite the dense deployment of Tx's in Fig. 2d, there are always interference "holes" at equal distance from the nearby Tx's, where the interference level is low. However, the intuition is that the aggregate signal power measured at the "holes" should be relatively high due

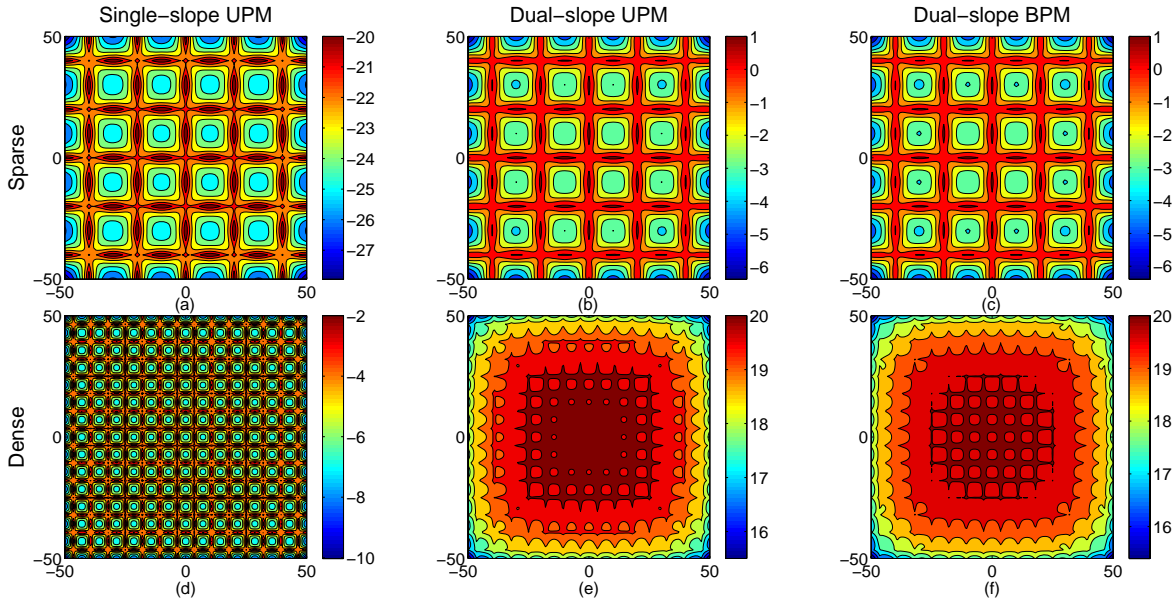


Figure 2. Interference power (in dBmW) in the two-dimensional square of side length 50 m. Tx's are located on the fixed grid of the same interval with Tx power 20 dBmW. Tx density is 3.6×10^3 BS/km² in (a), (b) and (c), and 2.5×10^5 BS/km² in (d), (e) and (f). In (a) and (d), single-slope UPM [13] is applied with $\alpha = 4$. In (b) and (e), dual-slope UPM [5] is applied with $\alpha_0 = 2$ and $\alpha_1 = 4$. In (c) and (f), dual-slope BPM is applied with $\alpha_0 = 2$ and $\alpha_1 = 4$. Note that $h_{Tx} = h_{Rx} = 1$ m and $\lambda = 0.15$ m (over subcarrier $f_c = 900$ MHz) such that $R_C = \frac{4h_{Tx}h_{Rx}}{\lambda} = 12.5$ m. In addition, small-scale fading is considered such that a fair comparison can be made.

to addition of LoS and reflection waves within critical distance, as shown in Figs. 2e and 2f using the dual-slope model. Meanwhile, it is observed from the central area of the considered scenario that the interference level in Fig. 2f is more moderate than that in Fig. 2e. As explained, the reason is that the unbounded model artificially magnifies signal power close to Tx's. Although negligible in sparse networks, the influence scales with the network density and will eventually alter the spatial throughput scaling behavior, which is illustrated in the following.

B. Interpret Ultra-Densification From Spatial Throughput Perspective

Based on (2), we investigate the spatial throughput of an outdoor downlink cellular network. Specifically, we plot the spatial throughput defined in (2) varying with BS density in Fig. 3. Note that dual-slope UPM [5] and dual-slope BPM, which is suggested above, are applied to characterize the channel power gain caused by pathloss in the outdoor scenarios, respectively. It is observed in Fig. 3 that identical results are obtained using UPM and BPM when BS density is

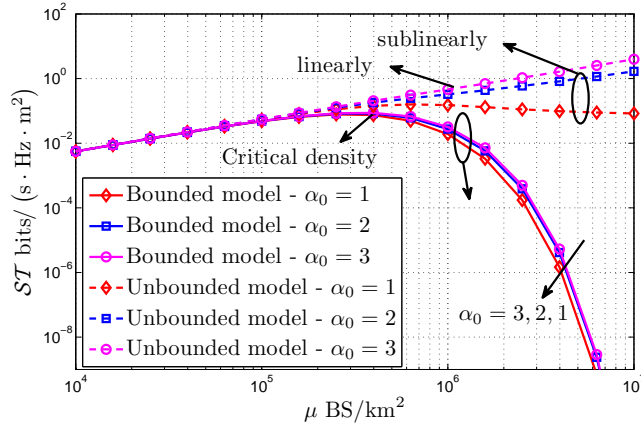


Figure 3. Spatial throughput scaling with BS density μ ($\tau = 0$ dB). Users are connected to the geometrically nearest BSs, which are assumed to be distributed according to a Poisson point process. Meanwhile, user density is much larger than the BS density to guarantee that each BS is associated with at least one user. The results under the unbounded model are obtained according to [5]. Therefore, we set $R_C = 1$ m and $\alpha_1 = 4$ to keep consistency with the results in [5]. Note that Rayleigh fading is applied to model small scale fading and the impact of noise is ignored, as noise is negligible compared to interference especially when BS density is large.

low. The reason is that little difference exists in modeling channel gains caused by pathloss using the two models when transmission distance is relatively large (also see Fig. 1). Nevertheless, we notice that the network performance is increasingly over-estimated using UPM. In particular, it is shown in Fig. 3 that the spatial throughput scales sublinearly with μ if $\alpha_0 \in [1, 2]$ and even scales linearly with μ if $\alpha_0 > 2$. In contrast, our results derived using BPM indicate that the throughput scales with rate $\mu e^{-\kappa\mu}$, i.e., first increases with μ and then decreases with μ [14]. Note that κ is a function of system parameters. In other words, network densification would degrade spatial throughput when BS density is sufficiently large. Accordingly, we characterize ultra-densification in terms of the spatial throughput scaling behavior.

Ultra-densification: Wireless networks are considered *ultra-dense* when the network density is larger than the *critical density*, beyond which system spatial throughput begins to decay. The network density has different interpretations in different network architectures. For instance, it refers to BS density in cellular uplink/downlink networks, while refers to density of activated Tx's in D2D networks.

Table II shows the critical densities under typical system settings, which are derived by making an extension of the results in [14]. Under the dual-slope BPM with $\alpha_1 = 3.5$, we observe that

SINR Threshold τ (dB)	μ_1^* (BS/km ²) $\alpha_0 = 2$ $\alpha_1 = 3$	μ_2^* (BS/km ²) $\alpha_0 = 2$ $\alpha_1 = 3.5$	μ_3^* (BS/km ²) $\alpha_0 = 2$ $\alpha_1 = 4$
0	2.0×10^5	2.51×10^5	3.16×10^5
5	7.94×10^4	1.26×10^5	1.59×10^5
10	3.16×10^4	6.31×10^4	7.94×10^4
15	1.58×10^4	3.16×10^4	5.01×10^4
20	6.3×10^3	1.58×10^4	2.51×10^4

Table II. Critical density μ^* for empirical pathloss exponent settings [15]. Note that dual-slope BPM is applied as the pathloss model, which is obtained by setting $N = 2$ in (1).

up to 6.31×10^4 BSs can be deployed per square kilometer to maximize the spatial throughput when $\tau = 10$ dB. Otherwise, if more BSs are deployed, the detriment of resulting inter-cell interference overwhelms the benefits of spatial reuse, which degrades spatial throughput. In this case, provided that 1 million connections/km² are to be supported in the places such as open gathering [1], almost 16 connections are served by each BS. Meanwhile, if users demand for higher transmission rate or equivalently greater SINR threshold, the critical BS density is reduced. For instance, under the dual-slope BPM with $\alpha_1 = 3.5$ and $\tau = 20$ dB, the critical density is 1.58×10^4 BS/km². This is because the transmission with higher rate is vulnerable and more likely to be interrupted by inter-cell interference. In addition, we observe from Table II that larger pathloss exponents lead to larger critical densities. In particular, the critical density increases to 2.51×10^4 BS/km² under the dual-slope BPM with $\alpha_1 = 4$ and $\tau = 20$ dB. The reason is that interference would decay more quickly with distance under larger pathloss exponents. As a result, its influence on spatial throughput is weakened. Note that the empirical pathloss exponents are basically large in urban areas, where the building blocks either form a regular Manhattan type of grid or have more irregular locations [15].

The above results also confirms the importance of applying multi-slope BPM to model the channel power gain in ultra-dense scenarios. Despite capturing the different power decay rates over different distances, multi-slope UPM fails to capture the power loss within near-field regions and it even artificially enhances the received power when $d \in (0, 1)$ m. This makes the increase of aggregate interference power be counter-balanced by the increase of the desired signal

power. Consequently, the successful probability in (2) is over-estimated and spatial throughput linearly/sublinearly increases with μ . Instead, the multi-slope BPM is capable of characterizing moderate power decay within near-field region and $(0, 1)$ m, which is consistent with practice (see Fig. 1). Under BPM, the spatial throughput is shown to be eventually degraded by the over-deployment of BSs. Therefore, the results indicate that multi-slope BPM can serve as a reasonable pathloss model especially in UDN.

IV. CHALLENGES TOWARDS INTERFERENCE MANAGEMENT AND POSSIBLE SOLUTIONS IN UDN

Aided by the interpretation of ultra-densification, we have been fully aware of the fact that over-deployment of BSs/APs and over-activation of devices indeed degenerate the performance of wireless networks. The reason is that the complicated signal propagation features would render interference distribution in UDN highly location-dependent. This leads to new challenges in the implementation of the state-of-the-art techniques in UDN, such as air interface design, resource management and interference management, etc., which are basically designed for sparse scenarios. Among them, interference management obviously bears the brunt, as it has the intrinsic potential to handle the overwhelming interference in UDN. In this part, we elaborate the challenges of interference management brought by ultra-densification and then provide possible solutions. Furthermore, a tailored ICA strategy is designed to combat interference for ultra-dense scenarios.

A. Challenges and Solutions to Implement Interference Management

To realize efficient interference management in UDN, there are issues and challenges to be considered and well addressed. We highlight some of them in the following. Besides, possible solutions are sketched to offer future research directions.

1) *Unavoidable Interference*: As user demand is always increasing, operators and vendors in competition are likely to allocate more resources, for instance, over-deploying more small-cell BSs and purchasing more frequency bands, etc. However, it is shown that simply increasing the

amount of resources such as BS density would result in excessive interference, which eventually degrades system performance (see Fig. 3). Therefore, how to handle the unavoidable interference remains to be settled.

As the main driver to interference in UDN is the service generated by users, we introduce the concept of service-oriented interference management. The motivation behind this is that service requirements are readily to be estimated due to the time and spatial correlation of user behavior in UDN. Hence, the interference distribution may be forecast and estimated as well. Accordingly, resources can be reserved in advance for the overcrowded places and the concept of cross-layer design can be adopted for joint optimization, thereby making interference management service-oriented.

2) *Loss of Channel Independence*: Network densification makes the channels of transmission pairs in close proximity become spatially correlated. However, the design of many interference management strategies is based on the channel independence assumption. For instance, IA precoders are designed provided that the channels generated by multiple antennas are uncorrelated. If channels are partially dependent, more antennas are needed to design the precoders, which renders IA cost-inefficient. Worststill, if channels are entirely dependent, precoders cannot be designed and IA would totally lose its merit in interference mitigation.

There are two directions that may be helpful to address this problem. One is to use channel-correlation-aware clustering method. As an example, the coordination clusters can be formed based on the location information of the transmission pairs involved to ensure that their mutual channels are less correlated. Another direction is to design joint resource allocation and interference management method. For instance, the identical spectrum resources can be allocated to the transmission pairs, which are located apart from each other. In consequence, the signals conveyed over the same spectrum resources are less dependent. Besides, the target of resource allocation can be minimizing the channel correlation coefficients, thereby enhancing the performance of interference coordination.

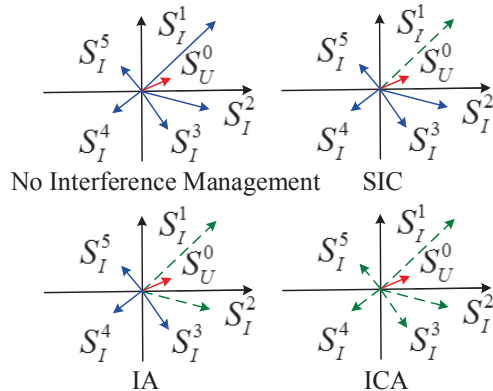
3) *Narrowed Interference Level*: In dense networks, interference signals basically stem from the interferers, which are geometrically close to the intended Rx. Accordingly, the interference

levels become less divergent. Nevertheless, for strategies such as interference cancellation, large divergence of interference levels is required such that interference can be more easily decoded, reconstructed and canceled. Therefore, the performance of interference cancellation may be significantly degraded.

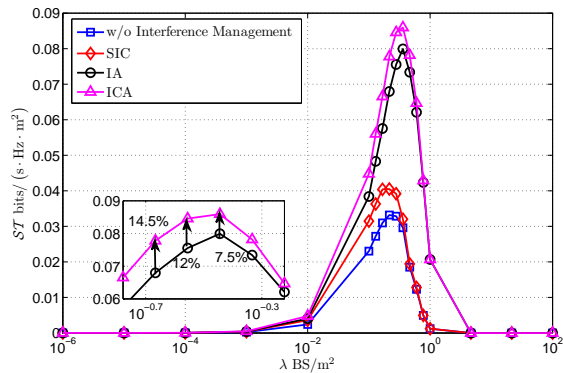
In order to re-activate interference cancellation in UDN, it's necessary to integrate it with other schemes. Here, we provide two possible approaches. a) Power control can be combined with interference cancellation. Specifically, the strength of desired signal and interference signal can be controlled using well designed power control method. Therefore, large power divergence can be more easily obtained. b) Interference cancellation can be jointly designed with resource allocation. For instance, identical spectrum resources can be assigned to the cluster of transmission pairs, whose mutual interference levels are of large divergence, so as to satisfy the cancellation constraints within the cluster. Note that the mutual interference levels can be obtained using channel estimations.

B. A Novel Interference Management Strategy for UDN

To breakthrough the performance limitation brought by network ultra-densification, we propose an ICA strategy, which flexibly integrates SIC and IA. The basic principle of ICA is to use IA to cancel the interference, which is not strong enough and cannot be canceled using SIC. Accordingly, the cancellation constraints of SIC are easier to be satisfied. We illustrate the benefits of ICA in Fig. 4a. Fig. 4a shows the received signals at Rx_0 . Specifically, besides the desired signal S_U^0 from Tx_0 , Rx_0 receives interference signals S_I^i from Tx_i ($i = 1, \dots, 5$) as well. It is assumed that 2 antennas are equipped on each Tx/Rx and the signal strength follows $S_I^i < S_I^j$ if $i > j$. Meanwhile, we further assume that S_I^1 , S_I^3 and S_I^5 can be successively canceled if without S_I^2 and S_I^4 . Therefore, only S_I^1 can be canceled using SIC, and S_I^1 and S_I^2 can be canceled using IA. In contrast, when ICA is used, Tx_0 would collaborate with Tx_2 and Tx_4 to form an IA-cluster for joint precoder design. In the ideal case, S_I^2 and S_I^4 can be projected into the orthogonal space with S_U^0 using IA and hence their influence on the reception of S_U^0 is mitigated. Then, the SIC decoder equipped on Rx_0 can be used to successively cancel S_I^1 , S_I^3



(a) Illustration of benefits of ICA.



(b) Spatial throughput scaling with BS density.

Figure 4. ICA strategy. In (a), S_U^0 and S_I^i ($i = 1, \dots, 5$), respectively, denote the useful signal and interference signal received by the intended Rx. In (b), system parameters are set as $R_C = 1$ m, $\alpha_0 = 2$, $\alpha_1 = 4$ and $\tau = 0$ dB. Two antennas are assumed to be equipped on Tx's and Rx's.

and S_I^5 .

Fig. 4b shows spatial throughput varying BS density when SIC, IA and ICA are applied, respectively. We observe that the performance of the three strategies is comparable at low BS densities. The reason is that the divergence between strong and weak interference is so large that canceling strong interference would greatly improve the user performance, which can be done using any of the three strategies. However, when the BS density becomes larger, the gap between spatial throughput achieved by SIC and that achieved by ICA increases. More importantly, the critical density achieved by ICA is greater than that achieved using SIC. Besides, ICA always outperforms IA (13% gain on average and 7.5% gain at the critical density). The results indicate that ICA can be applied into the scenarios with higher density.

V. CONCLUSION REMARKS

Network densification is an inevitable tendency in future wireless networks, which significantly reduces transmission distance and make signal propagation transit from far- to near-field propagation. In this article, we discuss the impact of near-field propagation on the wireless network performance, especially considering densely deployed scenarios. Remarkably, we found that network densification would eventually drain the spatial resources and degrade network

performance when network density exceeds a critical density. More importantly, aided by the critical density, we demonstrate how dense is ultra-dense from the perspective of spatial throughput scaling law. The result serves as a guidance for network deployment, as it indicates under what circumstances deploying more BSs/APs is beneficial to enhancing network capacity.

Network densification has raised new challenges and opportunities to the state-of-the-art wireless communications techniques, besides interference management. For instance, resource management is to be rethought in UDN. The primary reason is that the over-deployment of BSs and over-activation of devices would exponentially increase the overhead for resource management. Therefore, how to strike a good balance between network performance and the resulting overhead becomes more critical in UDN. In summary, this article has merely shed light on a drop in the bucket of UDN. It is imperative to fully understand and exploit the inherent features of UDN, thereby achieving the aggressive goals of future wireless networks.

REFERENCES

- [1] IMT-2020 (5G) Promotion Group, “5G vision and requirements,” Tech. Rep., Dec. 2015. [Online]. Available: <http://www.imt-2020.org.cn/en/documents/download/3>
- [2] W. Webb, *ArrayComm*. London, U.K.: Ofcom, 2007.
- [3] P. K. Agyapong, M. Iwamura, D. Staehle, W. Kiess, and A. Benjebbour, “Design considerations for a 5G network architecture,” *IEEE Commun. Mag.*, vol. 52, no. 11, pp. 65–75, Nov. 2014.
- [4] S. Chen, F. Qin, B. Hu, X. Li, and Z. Chen, “User-centric ultra-dense networks for 5G: challenges, methodologies, and directions,” *IEEE Wireless Commun.*, vol. 23, no. 2, pp. 78–85, April 2016.
- [5] X. Zhang and J. G. Andrews, “Downlink cellular network analysis with multi-slope path loss models,” *IEEE Trans. Commun.*, vol. 63, no. 5, pp. 1881–1894, May 2015.
- [6] M. Ding, P. Wang, D. Lopez-Perez, G. Mao, and Z. Lin, “Performance impact of LoS and NLoS transmissions in dense cellular networks,” *IEEE Trans. Wireless Commun.*, vol. 15, no. 3, pp. 2365–2380, Mar. 2016.
- [7] M. J. Cho, T. W. Ban, B. C. Jung, and H. J. Yang, “A distributed scheduling with interference-aware power control for ultra-dense networks,” in *Proc. IEEE ICC*, London, UK, Jun. 2015, pp. 1661–1666.
- [8] Z. Zhou, M. Dong, K. Ota, and Z. Chang, “Energy-efficient context-aware matching for resource allocation in ultra-dense small cells,” *IEEE Access*, vol. 3, pp. 1849–1860, Sep. 2015.
- [9] J. G. Andrews, X. Zhang, G. D. Durgin, and A. K. Gupta, “Are we approaching the fundamental limits of wireless network densification?” *submitted to IEEE Commun. Mag.*, 2015. [Online]. Available: <http://arxiv.org/abs/1512.00413>
- [10] H. Inaltekin, M. Chiang, H. V. Poor, and S. B. Wicker, “On unbounded path-loss models: effects of singularity on wireless network performance,” *IEEE J. Sel. Areas Commun.*, vol. 27, no. 7, pp. 1078–1092, Sep. 2009.

- [11] R. K. Ganti and M. Haenggi, "Interference and outage in clustered wireless ad hoc networks," *IEEE Trans. Inf. Theory*, vol. 55, no. 9, pp. 4067–4086, Sep. 2009.
- [12] H. Inaltekin, "Gaussian approximation for the wireless multi-access interference distribution," *IEEE Trans. Signal Process.*, vol. 60, no. 11, pp. 6114–6120, Nov. 2012.
- [13] H. S. Dhillon, R. K. Ganti, F. Baccelli, and J. G. Andrews, "Modeling and analysis of K-Tier downlink heterogeneous cellular networks," *IEEE J. Sel. Areas Commun.*, vol. 30, no. 3, pp. 550–560, Apr. 2012.
- [14] J. Liu, M. Sheng, L. Liu, and J. Li, "Effect of densification on cellular network performance with bounded pathloss model," *submitted to IEEE Commun. Lett.*, 2016. [Online]. Available: <http://arxiv.org/abs/1606.01599>
- [15] P. Kyösti, J. Meiniälä, L. Hentilä, X. Zhao, T. Jämsä, C. Schneider, M. Narandzic, M. Milojevic, A. Hong, J. Ylitalo *et al.*, "Winner II channel models," *WINER II Public Deliverable*, pp. 42–44, 2007.